



Role of activating transcription factor 3 in fructose-induced metabolic syndrome in mice

Chu-Lin Chou¹ · Ching-Hao Li^{2,3} · Heng Lin^{2,4} · Mei-Hui Liao⁵ · Chin-Chen Wu⁵ · Jin-Shuen Chen¹ · Yuh-Mou Sue^{6,7} · Te-Chao Fang^{7,8}

Received: 24 September 2017 / Revised: 13 December 2017 / Accepted: 7 January 2018 / Published online: 12 June 2018
© The Japanese Society of Hypertension 2018

Abstract

Activating transcription factor 3 (ATF3) has been implicated in cardiovascular disease and inflammation. This study examined the effects of ATF3 knockout (KO) on blood pressure, glucose intolerance, dyslipidemia, inflammation, and visceral adiposity in mice fed who did and did not consume a high-fructose diet. Male mice were divided into four groups ($N = 15$ for each group): the Con (control) group (wild-type mice fed a standard chow diet), Fru group (wild-type mice fed a high-fructose [60% fructose] diet), ATF3KO-Con group (ATF3 KO mice fed a standard chow diet), and ATF3KO-Fru group (ATF3 KO mice fed a high-fructose [60% fructose] diet). Experiments were conducted for 8 weeks. Our data demonstrated that ATF3 KO mice have lower systolic blood pressure (SBP) levels than do wild-type mice, and that high-fructose diets increase SBP levels in both wild-type and ATF3 KO mice. ATF3 KO in mice increased the serum levels of glucose, insulin, triglycerides, tumor necrosis factor-alpha, and intercellular adhesion molecule-1, impaired endothelium-dependent aortic relaxation, increased aorta wall thickness and lipid peroxide, and expanded visceral adiposity. These symptoms resembled those exhibited by the wild-type mice fed a high-fructose diet, which caused hyperglycemia, insulin resistance, dyslipidemia, endothelium-dependent aortic dysfunction, inflammation, aorta remodeling, and visceral adiposity. A high-fructose diet among ATF3 KO mice deteriorated metabolic parameters and inflammatory cytokines. The present results therefore suggest that ATF3 deficiency is involved in the pathogenesis of metabolic syndrome and ATF3 might have a therapeutic role in fructose-induced impairment of endothelium-dependent aortic relaxation, a rising of inflammatory cytokines, and metabolic syndrome.

These authors contributed equally: Chu-Lin Chou, Ching-Hao Li

This study will be presented at the 2017 Annual Meeting and Conference (Taipei, 2–3 December 2017), Taiwan Society of Internal Medicine.

Electronic supplementary material The online version of this article (<https://doi.org/10.1038/s41440-018-0058-9>) contains supplementary material, which is available to authorized users.

✉ Yuh-Mou Sue
sueym@tmu.edu.tw

✉ Te-Chao Fang
fangtechao@gmail.com

¹ Division of Nephrology, Department of Internal Medicine, Tri-Service General Hospital, National Defense Medical Center, Taipei, Taiwan

² Department of Physiology, School of Medicine, College of Medicine, Taipei Medical University, Taipei, Taiwan

³ Graduate Institute of Medical Sciences, College of Medicine, Taipei Medical University, Taipei, Taiwan

Introduction

Metabolic syndrome is marked by increased blood pressure, blood sugar levels, and body fat weights around the waist, as well as blood triglycerides levels, which increase the risk of cardiovascular disease and stroke [1, 2]. Similarly, a high-fructose (60% fructose) diet in rodents

⁴ College of Pharmacy, Taipei Medical University, Taipei, Taiwan

⁵ Graduate Institute of Medical Sciences, National Defense Medical Center, Taipei, Taiwan

⁶ Division of Nephrology, Department of Internal Medicine, Wan Fang Hospital, Taipei Medical University, Taipei, Taiwan

⁷ Division of Nephrology, Department of Internal Medicine, School of Medicine, College of Medicine, Taipei Medical University, Taipei, Taiwan

⁸ Division of Nephrology, Department of Internal Medicine, Taipei Medical University Hospital, Taipei Medical University, Taipei, Taiwan

causes high blood pressure, hyperglycemia, insulin resistance, and dyslipidemia. In addition, this diet exacerbates the activity of the renin–angiotensin system (RAS) [3, 4]. Our previous studies have also observed these phenomena in fructose-fed hypertensive rodents [5, 6]. Therefore, animal models of fructose-fed rodents have commonly been used to investigate hypertension and metabolic disturbances [7–9].

Activating transcription factor 3 (ATF3) is a member of the ATF/cAMP responsive element-binding protein family of transcription factors with the basic region-leucine zipper (bZip) DNA-binding domain [10]. The cDNA of ATF3 was originally isolated in 1989 [11]. In combination with a homodimer and various heterodimers with other bZip proteins, such as ATF2, c-Jun, JunB, and JunD, ATF3, can function as a transcriptional activator or repressor [12]. Adaptive-response transcription factors play a crucial role in cellular adaptation to maintain physiological homeostasis. ATF3 is a hub of the cellular adaptive-response network, and is induced under various stress and inflammatory conditions. Furthermore, ATF3 functions as an early responder to connect various signaling pathways to downstream events.

Our previous study on fructose-fed rodents with metabolic syndrome revealed that RAS inhibition could not only prevent and ameliorate metabolic syndrome [5], but also improve aortic endothelial functions and oxidative stress [6]. Lin et al. showed that compared with wild-type mice, ATF3 KO mice have decreased left ventricular contractility, decreased normal cardiac hypertrophic remodeling, and increased apoptosis [13]. Furthermore, ATF3 could play a role in cardiovascular disease. However, the role of ATF3 in metabolic syndrome remains under investigation. Therefore, the present study elucidated the role of ATF3 KO on blood pressure, glucose intolerance, dyslipidemia, endothelium-dependent aortic relaxation, and visceral adiposity in mice who did and did not consume a high-fructose diet.

Methods

Animals

All experimental procedures were approved by the Institutional Animal Care and Use Committee of Taipei Medical University (Protocol Number: LAC-2016-0093) and were in strict accordance with the recommendations of the Guide for the Care and Use of Laboratory Animals set by the National Institutes of Health. Male wild-type mice (C57BL/6J) and ATF3 KO mice (a gift from Dr. Tsonwin Hai to Dr. Heng Lin) were maintained in a room at 24 °C–27 °C, with 50–80% humidity and 12-h light/dark cycle; the mice had

access to tap water ad libitum throughout the experiments. After a control period of 1 week, the mice were divided into four groups ($N = 15$ for each group): the Con (control) group (wild-type mice fed a standard chow diet), Fru group (wild-type mice fed a high-fructose [60% fructose] diet), ATF3KO-Con group (ATF3 KO mice fed a standard chow diet), and ATF3KO-Fru group (ATF3 KO mice fed a high-fructose [60% fructose] diet). The experiments were conducted for 8 weeks.

The high-fructose feed (Harlan Teklad, Madison, WI, USA) was composed of 60% fructose, 21% protein, 5% fat, 8% cellulose, and a standard vitamin and mineral mix. The standard chow diet was composed of 50% starch, 21% protein, 4% fat, 4.5% cellulose, and a standard vitamin and mineral mix.

The first day of fructose feeding was defined as Day 1. Body weight (BW) was measured twice a week, and SBP levels were also measured twice a week using the tail-cuff method. Mice were killed on Day 0 ($N = 5$) and Day 56 ($N = 10$). Blood samples (1.5 mL) were obtained after 12 h of fasting on Day 0 and at the end of the study period (Day 56). Blood samples were collected in ethylenediaminetetraacetic-acid-containing tubes and immediately placed in an ice bath (2–4 °C). To assess insulin resistance, the intraperitoneal glucose tolerance test (IGTT) was performed on Day 55.

ATF3 KO mice

ATF3 KO mice were provided by Dr. Tsonwin Hai (Ohio State University, OH, USA). The ATF3 KO allele was backcrossed into C57BL/6 mice for at least seven generations before the fructose-feeding experiments. The generation and confirmation of ATF3 KO mice was performed as described previously [14]. Genotyping was performed using the polymerase chain reaction. Specifically, the following three primers were used: 5'-AGAGCTTCAGCAATGGTT TGC-3' (primer 1), 5'-TGAAGAAGGTAAACACACCCG TG-3' (primer 2), and 5'-ATCAGCAGCCTCTGTTCCA C-3' (primer 3).

SBP measurements

The tail-cuff method was used to measure SBP levels using a programmed electrosphygmomanometer (model UR-5000, Ueda) as described previously [15, 16]. In brief, mice were removed from the animal room and taken to the laboratory at 8 am; they were allowed free access to water and were kept in a quiet area before SBP measurements at 9 am. The mean of six consecutive readings was considered the SBP of each mouse for a particular day. SBP levels were measured twice a week during both the control (1 week) and experimental (8 weeks) periods.

IGTT

The IGTT was performed on Day 55. After a 12-h fasting period, 0.1 mL of blood was collected from the tail vein, and blood glucose levels were measured using a standard glucometer (Bayer, Leverkusen, Germany). Immediately after the baseline measurement, a hydrous solution of 2.0 g glucose/kg BW was administered intraperitoneally as described by Zmuda et al. [17]. Blood glucose levels were measured at 0, 30, 60, and 120 min after intraperitoneal glucose loading.

Laboratory investigations

The blood samples were immediately centrifuged at $4000 \times g$ at 4°C for 10 min. The serum levels of glucose, triglycerides, and total cholesterol were assayed using an automated analyzer of an enzymatic colorimetric reaction (Olympus AU 270, Hamburg, Germany). The serum levels of insulin (Mercodia AB, Uppsala, Sweden), tumor necrosis factor- α (TNF- α ; Raybiotech, Norcross, GA), and intercellular adhesion molecule-1 (ICAM-1; Raybiotech, Norcross, GA) were measured using commercially available enzyme-linked immunosorbent assay kits.

In vitro vascular reactivity

The isolated rings of the thoracic aortas were obtained from the four groups of mice for analysis of endothelium-dependent vascular contraction at Day 56. The thoracic aortas were dissected and aortic ring segments (3 mm in length) were suspended in individual organ chambers and in vitro vascular reactivity was assessed as described in our previous studies [6, 18]. The active muscle tone of ring segments was then appropriately contracted by phenylephrine. After a stable contraction plateau was reached, relaxation of the aortic rings was measured in response to cumulative additions of acetylcholine (ACh, Sigma; 10^{-9} – 10^{-4} mol/L). After the last vasodilator response to acetylcholine, a single dose of NG-nitro-L-arginine methyl ester (L-NAME; 100 nmol), a nitric oxide (NO) synthesis inhibitor, was applied. When a steady contraction in response to phenylephrine and L-NAME was reached, the vasodilator response to sodium nitroprusside (SNP, Riedel-deHaen, Seelze, Germany; 10^{-9} – 10^{-4} mol/L) was evaluated.

Remodeling of the aortic wall

Briefly, 3- μm -thick paraffin-embedded specimens of thoracic aorta were stained with hematoxylin–eosin. Vascular wall thickness was measured as an indicator of structural abnormalities of the aorta. Histopathology and

morphometry was performed by investigators who were blinded to the treatment being administered. An average of ten measurements of aortic wall (diameter, μm) was taken as each individual value.

Analysis of oxidative stress marker in aorta

The lipid peroxide level, a marker for oxidative stress, in the thoracic aortic tissue was assessed by measuring thio-barbituric acid reactive substances (TBARS) using a commercially available kit (Cell Biolabs, San Diego, CA, USA). TBARS values were expressed as nmol/mg of protein.

Measurement of the weight of visceral fat pads and other visceral organs

On Day 56, retroperitoneal, mesenteric, epididymal fat pads, and visceral organs (heart, liver, and kidneys) were rapidly dissected and weighed. We measured the weights of the fat pads and visceral organs, which were normalized to BW (g/g, %).

Analysis of angiotensin II (Ang II) levels

To measure Ang II values in the visceral fat pads (retroperitoneal, mesenteric, and epididymal tissue), adipose samples (0.3 mg) were homogenized at 4°C in tissue extraction buffer (0.6 mL) for 15 min. The tissue extraction buffer was a commercially available buffer consisting of 29.4 mL T-PER[®] tissue protein extraction reagent (Thermo Scientific, USA), 300 μL Halt[™] protease and phosphatase inhibitor cocktail (Thermo Scientific, USA) and 300 μL EDTA. After freezing with liquid nitrogen for 5 s, adipose samples were centrifuged at $10,000 \times g$ for 20 min. After centrifugation, 0.5 mL of the supernatant (below the fat layer) was assayed. For adipose Ang II levels, 0.5 mL of the supernatant was measured by a quantitative sandwich enzyme immunoassay technique using a commercially available Ang II kit (SPI Bio, Montigny le Bretonneux, France) following the manufacturer's instructions. Tissue protein quantitation was measured using a Pierce[™] BCA Protein Assay Kit (Thermo Scientific, USA). Ang II values were expressed as picogram mg^{-1} of protein.

Statistical analyses

All results are expressed as mean \pm standard deviation (SD). A one-way analysis of variance (ANOVA), followed by the Newman–Keuls post hoc test or one-way repeated-measures ANOVA, was performed for group comparisons. The changes in BW and food intake were analyzed through repeated-measures ANOVA. Additionally, a two-way ANOVA (first factor: treatment group; second factor: time

period) considering diet-type and drug treatment as factors was performed to compare the groups, such as with respect to SBP levels. The Student's *t* test was performed for unpaired data when appropriate, and $P < 0.05$ was considered statistically significant.

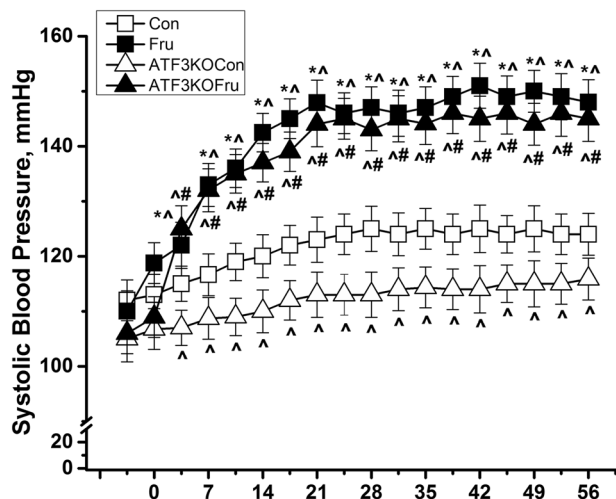
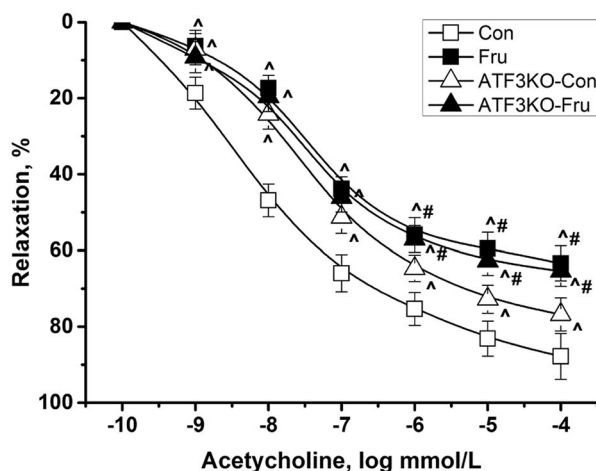


Fig. 1 Variations in SBP levels of mice who did or did not consume a high-fructose diet. Con: wild-type mice fed a standard chow diet; Fru: wild-type mice fed a high-fructose diet; ATF3KO-Con: ATF3 KO mice fed a standard chow diet; and ATF3KO-Fru: ATF3 KO mice fed a high-fructose diet. Values are presented as mean \pm SD. *, ^, and # denote $P < 0.05$ vs. the control period and the Con and ATF3KO-Con groups at the corresponding time point, respectively. $N = 10$ for each group



Results

In this study, the genotyping of DNA extracted from the tail tissues of mice showed that ATF3 expression was absent in ATF3 KO mice (Supplementary Figure 1). Furthermore, we examined the role of ATF3 KO on blood pressure, glucose intolerance, dyslipidemia, inflammation, and visceral adiposity in mice who did and did not consume a high-fructose diet.

Figure 1 shows the changes in systolic blood pressure (SBP) levels of control and fructose-fed mice. A high-fructose diet significantly increased SBP levels in both wild-type and ATF3 KO mice on Day 56, compared with control mice who were fed with a standard chow diet. However, SBP levels did not significantly differ between the Fru and ATF3KO-Fru groups. Furthermore, the ATF3KO-Con group had lower SBP levels than did the Con group, indicating that ATF3 deficiency could affect the blood pressure system.

The effects of ATF3 KO on endothelium-dependent relaxing responses to acetylcholine and sodium nitroprusside in aorta in mice who did or did not consume a high-fructose diet on Day 56 are shown in Fig. 2. The peak aortic relaxation induced by acetylcholine in the fructose-fed mice was significantly reduced compared with the control mice. The peak aortic relaxation in response to acetylcholine in the ATF3KO-Con group was significantly lower than those in the Con group ($76.76 \pm 4.36\%$ vs. $87.81 \pm 5.92\%$, respectively; $P < 0.05$). On the other hand, relaxation produced by sodium nitroprusside was not significantly different between these groups.

Table 1 presents the effects of ATF3 KO on the serum levels of glucose, insulin, triglycerides, total cholesterol,

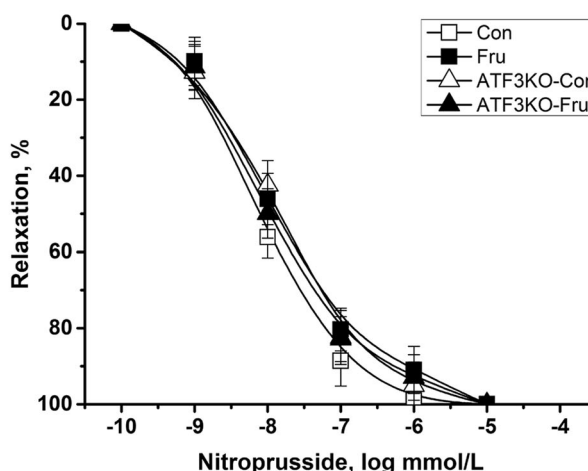


Fig. 2 Endothelium-dependent vascular relaxations in response to acetylcholine and endothelium-independent sodium nitroprusside in thoracic aortic segments in mice who did or did not consume a high-fructose diet on Day 56. Con: wild-type mice fed a standard chow diet; Fru: wild-type mice fed a high-fructose diet; ATF3KO-Con: ATF3 KO mice fed a standard chow diet; and ATF3KO-Fru: ATF3 KO mice fed

a high-fructose diet. Vessels were studied as ring segments in organ chambers, and relaxations in response to acetylcholine and sodium nitroprusside were measured. Values are presented as mean \pm SD. ^ and # denote $P < 0.05$ vs. the Con and ATF3KO-Con groups at the corresponding time point, respectively. $N = 10$ for each group

Table 1 Changes in the serum levels of glucose, insulin, triglycerides, total cholesterol, TNF- α , and ICAM-1 in mice fed with or without a high-fructose diet

Group	Day 0				Day 56			
	Con		Fru		ATF3KO-Con		ATF3KO-Fru	
	5	10	5	10	5	10	5	10
N	5	10	5	10	5	10	5	10
Glucose, mmol/L	4.49 \pm 1.23	4.52 \pm 1.37	4.50 \pm 1.35 [#]	4.52 \pm 1.37	8.00 \pm 1.16 ^{^, &}	8.05 \pm 1.27 ^{^, &}	8.00 \pm 1.54 ^{^, &}	11.96 \pm 1.91 ^{^, #}
Insulin, pmol/L	67.5 \pm 15.1	68.9 \pm 10.3	68.1 \pm 13.1 [#]	68.9 \pm 10.3	104.6 \pm 14.8 ^{^, &}	106.5 \pm 12.5 ^{^, &}	105.2 \pm 13.3 ^{^, &}	152.7 \pm 16.8 ^{^, #}
Triglycerides, mmol/L	0.45 \pm 0.06	0.46 \pm 0.07	0.44 \pm 0.09 [#]	0.46 \pm 0.07	0.70 \pm 0.08 ^{^, &}	0.83 \pm 0.08 ^{^, #}	0.69 \pm 0.07 ^{^, &}	0.97 \pm 0.09 ^{^, #}
Total cholesterol, mmol/L	1.86 \pm 0.22	1.87 \pm 0.26	1.85 \pm 0.26	1.87 \pm 0.26	1.89 \pm 0.28	3.10 \pm 0.29 ^{^, #}	1.88 \pm 0.25	3.39 \pm 0.24 ^{^, #}
TNF- α , pg/mL	6.22 \pm 0.43	6.57 \pm 0.43	6.31 \pm 0.49 [#]	6.57 \pm 0.43	8.21 \pm 0.64 ^{^, &}	8.27 \pm 0.57 ^{^, &}	8.15 \pm 0.52 ^{^, &}	11.87 \pm 0.60 ^{^, #, &}
ICAM-1, ng/mL	320 \pm 55	329 \pm 65	318 \pm 68 [#]	329 \pm 65	485 \pm 60 ^{^, &}	515 \pm 68 ^{^, &}	480 \pm 78 ^{^, &}	660 \pm 72 ^{^, #, &}

Con: wild-type mice fed a standard chow diet; Fru: wild-type mice fed a high-fructose diet; ATF3KO-Con: ATF3 KO mice fed a standard chow diet; and ATF3KO-Fru: ATF3 KO mice fed a high-fructose diet. Values are presented as mean \pm SD. ^, #, and & denote $P < 0.05$ vs. the Con, ATF3KO-Con, and Fru groups at the corresponding time point, respectively

N mice number

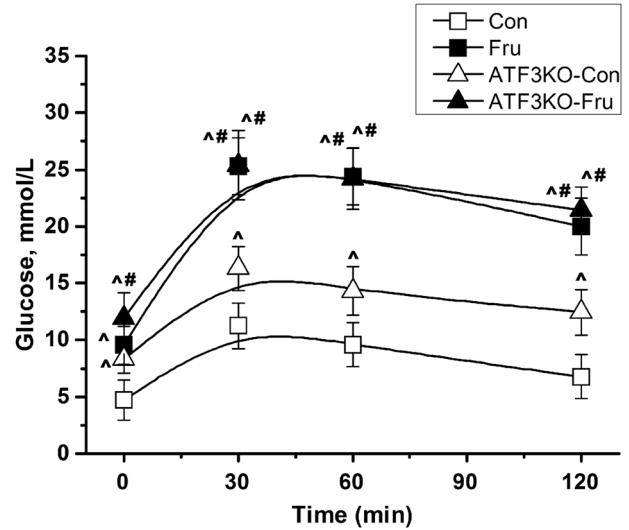


Fig. 3 Blood glucose curves following intraperitoneal glucose loading in mice who did or did not consume a high-fructose diet on Day 55. Con: wild-type mice fed a standard chow diet; Fru: wild-type mice fed a high-fructose diet; ATF3KO-Con: ATF3 KO mice fed a standard chow diet; and ATF3KO-Fru: ATF3 KO mice fed a high-fructose diet. After 12 h of fasting, a dose of 50% glucose solution (2 g/kg BW) was injected intraperitoneally. Values are presented as mean \pm SD. ^ and # denote $P < 0.05$ vs. the Con and ATF3KO-Con groups at the corresponding time point, respectively. $N = 10$ for each group

TNF- α , and ICAM-1. On Day 56, the serum levels of glucose, insulin, triglycerides, and total cholesterol were significantly increased in mice fed a high-fructose diet compared with those in the Con and ATF3KO-Con groups throughout the 56-day study period. Moreover, ATF3 KO mice had higher serum levels of glucose, insulin, and triglycerides than did wild-type mice, indicating the role of ATF3 in glucose, insulin, and triglyceride regulation in insulin resistance. Furthermore, on Day 56, the Fru and ATF3KO-Fru groups had significantly increased serum TNF- α and ICAM-1 levels compared with the Con and ATF3KO-Con groups. Furthermore, ATF3 KO mice had higher serum levels of TNF- α , and ICAM-1 than did wild-type mice, suggesting that ATF3 deficiency is an indicator of inflammation.

The response of serum glucose levels to intraperitoneal glucose loading was significantly higher in fructose-fed mice (i.e., the Fru and ATF3KO-Fru groups) than in normal diet-fed mice (i.e., the Con and ATF3KO-Con groups) (Fig. 3). Moreover, the ATF3KO-Con group significantly deteriorated the response of serum glucose levels to intraperitoneal glucose loading throughout the 2 h period, compared with the Con group (from 8.34 \pm 1.28 to 12.44 \pm 1.99 mmol/L and from 4.72 \pm 1.78 to 6.77 \pm 1.94 mmol/L, respectively).

The aortic wall remodeling and lipid peroxide levels in mice are presented in Fig. 4. Vascular wall hypertrophy and lipid peroxide levels were more significant in the ATF3KO-Con group than the Con group. Furthermore, mice on high-

fructose diets exhibited higher vascular wall thickness and

lipid peroxide levels in the aorta compared to mice on standard chow diet.

Visceral fat adiposity, such as epididymal and retroperitoneal fat pads, in ATF3 KO mice who did or did not consume a high-fructose diet were also noticeably enlarged, compared with those in control mice (Fig. 5a). Besides, the ratio of the other visceral organs weight over whole body weight (gram/gram, %) was not significantly different among these group, as showed in Supplementary Table 1.

Figure 5b shows the effect of fructose diet on Ang II levels in RAS activity. The Con and ATF3KO-Con groups had the equivalent Ang II expressions in the retroperitoneal, mesenteric, and epididymal fat pads. A high-fructose diet caused an increase in Ang II expression in the Fru and ATF3KO-Fru groups.

Discussion

The major findings of our study are summarized as follows. First, ATF3 KO mice have lower SBP levels than do wild-type mice, and high-fructose feeding increases SBP levels in wild-type and ATF3 KO mice. Second, ATF3 KO in mice increases the serum levels of glucose, insulin, triglycerides, TNF- α , and ICAM-1, impairs endothelium-dependent aortic relaxation, increases aorta wall remodeling and lipid peroxide levels, as well as expands visceral adiposity. These symptoms are similarly exhibited in wild-type mice who were fed with a high-fructose diet, and cause hyperglycemia, insulin resistance, dyslipidemia, inflammation, endothelium-dependent aortic dysfunction, aorta remodeling, oxidative stress, and visceral adiposity. Third, a high-fructose diet further deteriorates these metabolic parameters in ATF3 KO mice. Overall, these findings suggest that ATF3 deficiency is involved in the pathogenesis of metabolic syndrome and ATF3 might have a therapeutic role in fructose-induced impairment of endothelium-dependent aortic relaxation, a rising of inflammatory cytokines, and metabolic syndrome.

ATF3 has been implicated in the blood pressure and cardiovascular systems. Our data show that ATF3 KO mice have lower SBP levels than do wild-type mice may be due to ATF3 KO mice have decreased left ventricular contractility. Our previous study showed that, compared with wild-type mice, ATF3 KO mice have decreased left ventricular contractility with the loss of normal cardiac hypertrophic remodeling and increased apoptosis [13]. Furthermore, the infusion of tertbutylhydroquinone, a selective ATF3 inducer, in ATF3 KO mice increases ATF3 expression through the Nrf2 transcriptional factor, leading to improved cardiac dilatation and left ventricular contractility [13]. Zhou et al. showed that angiotensin-converting enzyme inhibitors improve blood pressure

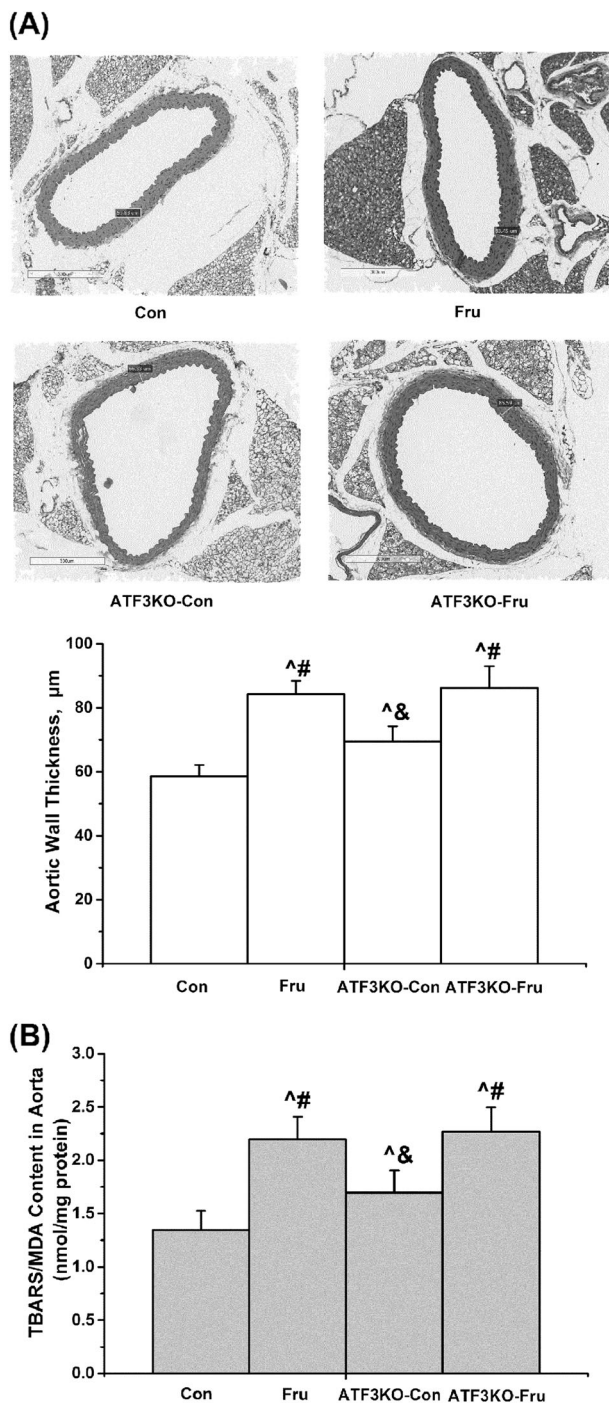


Fig. 4 Changes in **a** vascular remodeling and **b** lipid peroxide levels through measuring thiobarbituric acid reactive substances (TBARS) in the thoracic aorta in mice who did or did not consume a high-fructose diet on Day 56. Con: wild-type mice fed a standard chow diet; Fru: wild-type mice fed a high-fructose diet; ATF3KO-Con: ATF3 KO mice fed a standard chow diet; and ATF3KO-Fru: ATF3 KO mice fed a high-fructose diet. Hematoxylin–eosin staining in aorta. Values are presented as mean \pm SD. [^], [#], and [&] denote $P < 0.05$ vs. the Con, ATF3KO-Con, and Fru groups, respectively. $N = 10$ for each group

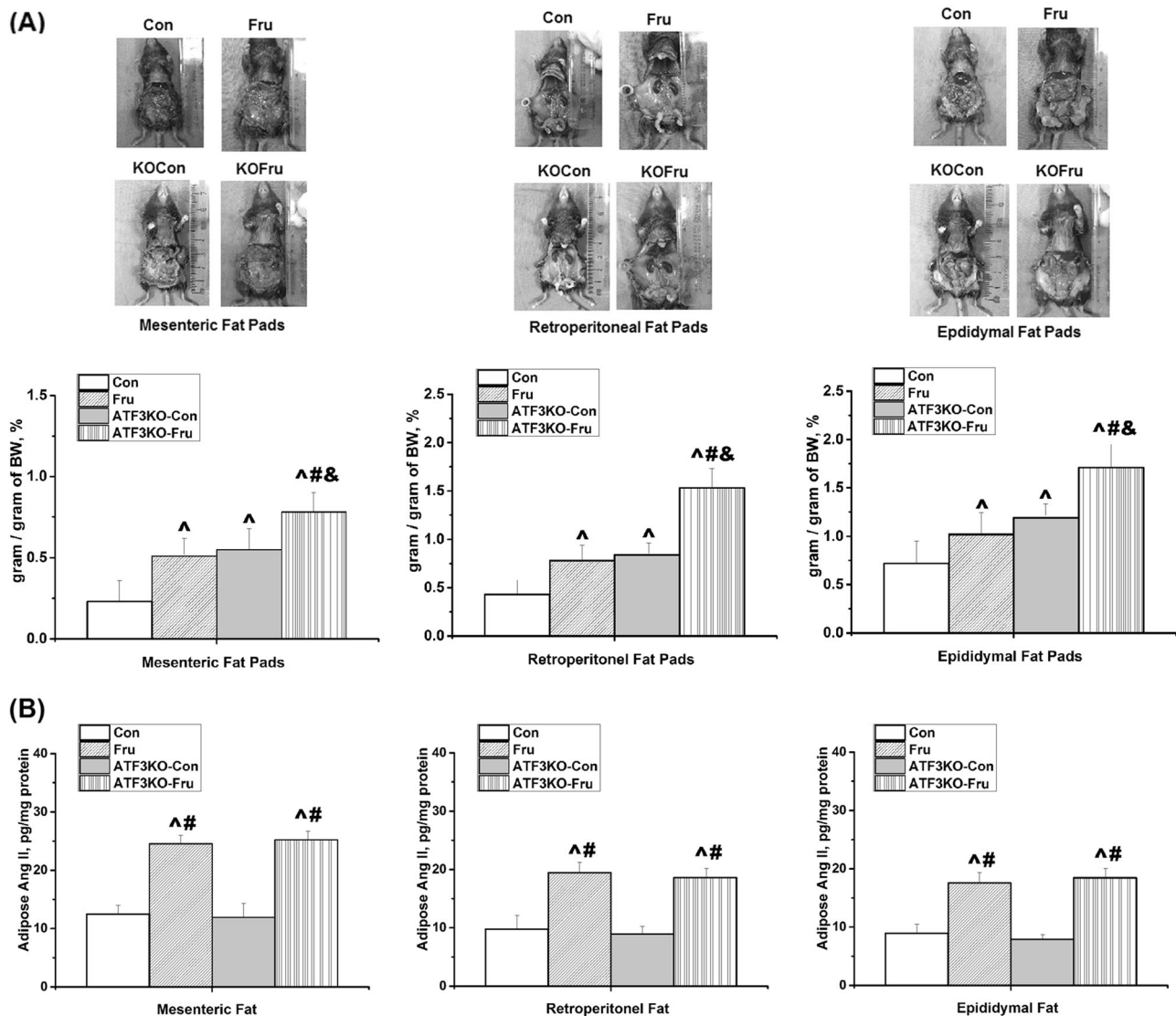


Fig. 5 Changes in **a** visceral fat adiposity and the ratio of visceral fat pad weight over the whole BW (g/g , %) and **b** angiotensin II values in mice who did or did not consume a high-fructose diet on Day 56. Con: wild-type mice fed a standard chow diet; Fru: wild-type mice fed a high-fructose diet; ATF3KO-Con: ATF3 KO mice fed a standard

chow diet; and ATF3KO-Fru: ATF3 KO mice fed a high-fructose diet. Values are presented as mean \pm SD. \wedge , #, and & denote $P < 0.05$ vs. the Con, ATF3KO-Con, and Fru groups, respectively. $N = 10$ for each group. BW body weight

levels in high homocysteine-associated hypertension by downregulating ATF3-mediated endoplasmic reticulum stress and oxidative stress in the aorta of rats [19]. These data imply that ATF3 can contribute in part to blood pressure regulation.

Until now, it remains unclear whether ATF3 could affect aortic endothelial function in mice. In this study, we evaluated the effect of ATF3 on endothelium-dependent aortic relaxation in mice with and without the high-fructose diet, and the results showed that ATF3 knock mice had the impairment of endothelium-dependent aortic relaxation compared with wild-type mice, which indicated that ATF3 has been implicated in regulating endothelial function. In a study of endothelial dysfunction in vitro, the results of

Teasdale et al. identify the importance of ATF3 as an important protective factor against endothelial dysfunction [20]. Moreover, ATF3 KO in mice had the increased aorta wall thickness and lipid peroxide levels, a marker of oxidative stress. Modulation of ATF3 expression may play a novel approach to modulate endothelial-dependent vascular function and vascular remodeling, and open new therapeutic viewpoints to treat cardiovascular diseases.

In this study, we observed that fructose diet caused the elevated SBP on the similar levels in wild-type mice and ATF3 KO mice. The reasons are that some recent studies [21–23], including our own study [6], have demonstrated that the RAS plays a major role in the pathogenesis of hypertension and vascular dysfunction in fructose-fed

rodents. A fructose diet in rats elevates plasma angiotensin II, activates the tissue angiotensin II type 1 receptor, leads to high blood pressure, impairs endothelial nitric oxide synthase, and results in vascular dysfunction [6, 22, 23]. This study considered a high-fructose diet to increase SBP levels in wild-type and ATF3 KO mice through the hypertensive effect of the RAS, as shown in Fig. 5b.

Our data also shows that high-fructose feeding in wild-type mice and ATF3 KO mice elevates the similar values of hyperglycemia, insulin resistance, and dyslipidemia. Moreover, fructose diet in those mice produces visceral adiposity. Those phenomena in high-fructose feeding are consistent with the findings of other studies [24–26]. Regarding lipogenic properties, excess fructose feeding causes glucose malabsorption and elevates triglyceride and cholesterol levels compared with other carbohydrates [27]. In addition, in this study, ATF3 deficiency in mice results in phenomena, such as elevated serum levels of glucose, insulin, triglycerides, inflammatory cytokines (TNF- α and ICAM-1), as well as larger visceral adiposity, resembling metabolic syndrome. Zmuda et al. reported that wild-type mice who were fed a normal diet had more favorable outcomes than did ATF3 KO mice who were also fed with a normal diet in the glucose tolerance test, hinting at the protective role of ATF3 in glucose tolerance [17]. ATF3-deficient mice are reported to develop hepatic steatosis [28]. Recently, Kalfon et al. reported that cardiac-specific ATF3 KO mice fed with a high-fat diet for 15 weeks experienced severe cardiac fibrosis and dysfunction, hyperglycemia, insulin resistance, and high inflammatory cytokine (interleukin-6 and TNF- α) levels compared with wild-type mice who were fed a high-fat diet [29]. A study on *Drosophila melanogaster* suggested that ATF3 deficiency results in chronic inflammation and metabolic disturbances [30].

In conclusion, our study shows that high-fructose feeding in wild-type and ATF3 KO mice results in a significant increase in SBP levels, the serum levels of glucose, triglycerides, and total cholesterol, impairment of endothelium-dependent aortic relaxation, progress of aorta wall thickness and lipid peroxide, and expansion of visceral adiposity, all of which resemble metabolic syndrome. Compared with wild-type mice, ATF3 KO in mice reduces SBP levels and increases the serum levels of glucose, insulin, triglycerides, TNF- α , ICAM-1, visceral adiposity, and aorta wall thickness and lipid peroxide, as well as reduces endothelium-dependent aortic relaxation. Moreover, high-fructose feeding in ATF3 KO mice deteriorates these metabolic parameters. These present results therefore suggest that ATF3 deficiency is involved in the pathogenesis of metabolic syndrome and ATF3 might have a therapeutic role in fructose-induced impairment of endothelium-dependent aortic relaxation, a rising of inflammatory cytokines, and metabolic syndrome.

Acknowledgements This work was supported by Wan Fang Hospital, Taipei Medical University, Taipei, Taiwan (105 TMU-WFH-06; funds for Y-MS), by Taipei Medical University (TMU103-AE1-B30; funds for T-CF) and by Ministry of Science and Technology, Taiwan (MOST 105-2314-B-038-024; funds for T-CF). The funder had no role in study design, data collection and analysis, publication decision, or manuscript preparation.

Compliance with ethical standards

Conflict of interest The authors declare that they have no conflict of interest.

References

1. Reaven GM. Banting lecture 1988. Role of insulin resistance in human disease. *Diabetes*. 1988;37:1595–607.
2. Lamounier-Zepter V, Ehrhart-Bornstein M, Bornstein SR. Insulin resistance in hypertension and cardiovascular disease. *Best Pract Res Clin Endocrinol Metab*. 2006;20:355–67.
3. Hwang IS, Ho H, Hoffman BB, Reaven GM. Fructose-induced insulin resistance and hypertension in rats. *Hypertension*. 1987;10:512–6.
4. Catena C, Cavarape A, Novello M, Giacchetti G, Sechi LA. Insulin receptors and renal sodium handling in hypertensive fructose-fed rats. *Kidney Int*. 2003;64:2163–71.
5. Chou CL, Lai YH, Lin TY, Lee TJ, Fang TC. Aliskiren prevents and ameliorates metabolic syndrome in fructose-fed rats. *Arch Med Sci*. 2011;7:882–8.
6. Chou CL, Pang CY, Lee TJ, Fang TC. Direct renin inhibitor prevents and ameliorates insulin resistance, aortic endothelial dysfunction and vascular remodeling in fructose-fed hypertensive rats. *Hypertens Res*. 2013;36:123–8.
7. Miatello R, Risler N, Gonzalez S, Castro C, Ruttler M, Cruzado M. Effects of enalapril on the vascular wall in an experimental model of syndrome X. *Am J Hypertens*. 2002;15:872–8.
8. Miatello R, Vazquez M, Renna N, Cruzado M, Zumino AP, Risler N. Chronic administration of resveratrol prevents biochemical cardiovascular changes in fructose-fed rats. *Am J Hypertens*. 2005;18:864–70.
9. Lee RM, Dickhout JG, Sandow SL. Vascular structural and functional changes: their association with causality in hypertension: models, remodeling and relevance. *Hypertens Res*. 2017;40:311–23.
10. Thompson MR, Xu D, Williams BR. ATF3 transcription factor and its emerging roles in immunity and cancer. *J Mol Med*. 2009;87:1053–60.
11. Hai TW, Liu F, Coukos WJ, Green MR. Transcription factor ATF cDNA clones: an extensive family of leucine zipper proteins able to selectively form DNA-binding heterodimers. *Genes Dev*. 1989;3:2083–90.
12. Hai T, Wolfgang CD, Marsee DK, Allen AE, Sivaprasad U. ATF3 and stress responses. *Gene Expr*. 1999;7:321–35.
13. Lin H, Li HF, Chen HH, Lai PF, Juan SH, Chen JJ, Cheng CF. Activating transcription factor 3 protects against pressure-overload heart failure via the autophagy molecule Beclin-1 pathway. *Mol Pharmacol*. 2014;85:682–91.
14. Hartman MG, Lu D, Kim ML, Kociba GJ, Shukri T, Buteau J, Wang X, Frankel WL, Guttridge D, Prentki M, Grey ST, Ron D, Hai T. Role for activating transcription factor 3 in stress-induced beta-cell apoptosis. *Mol Cell Biol*. 2004;24:5721–32.
15. Fang TC, Huang WC. Role of angiotensin II in hyperinsulinemia-induced hypertension in rats. *J Hypertens*. 1998;16:1767–74.

16. Fang TC, Huang WC. Angiotensin receptor blockade blunts hyperinsulinemia-induced hypertension in rats. *Hypertension*. 1998;32:235–42.
17. Zmuda EJ, Qi L, Zhu MX, Mirmira RG, Montminy MR, Hai T. The roles of ATF3, an adaptive-response gene, in high-fat-diet-induced diabetes and pancreatic beta-cell dysfunction. *Mol Endocrinol*. 2010;24:1423–33.
18. Chou CL, Pang CY, Lee TJ, Fang TC. Beneficial effects of calcitriol on hypertension, glucose intolerance, impairment of endothelium-dependent vascular relaxation, and visceral adiposity in fructose-fed hypertensive rats. *PLoS ONE*. 2015;10:e0119843.
19. Zhou Y, Zhao L, Zhang Z, Lu X. Protective effect of enalapril against methionine-enriched diet-induced hypertension: role of endoplasmic reticulum and oxidative stress. *Biomed Res Int*. 2015;2015:724876.
20. Teasdale JE, Hazell GG, Peachey AM, Sala-Newby GB, Hindmarch CC, McKay TR, Bond M, Newby AC, White SJ. Cigarette smoke extract profoundly suppresses TNF α -mediated proinflammatory gene expression through upregulation of ATF3 in human coronary artery endothelial cells. *Sci Rep*. 2017;7:39945.
21. Farah V, Elased KM, Chen Y, Key MP, Cunha TS, Irigoyen MC, Morris M. Nocturnal hypertension in mice consuming a high fructose diet. *Auton Neurosci*. 2006;130:41–50.
22. Shinozaki K, Ayajiki K, Nishio Y, Sugaya T, Kashiwagi A, Okamura T. Evidence for a causal role of the renin-angiotensin system in vascular dysfunction associated with insulin resistance. *Hypertension*. 2004;43:255–62.
23. Nyby MD, Abedi K, Smutko V, Eslami P, Tuck ML. Vascular angiotensin type 1 receptor expression is associated with vascular dysfunction, oxidative stress and inflammation in fructose-fed rats. *Hypertens Res*. 2007;30:451–7.
24. Choi Y, Abdelmegeed MA, Song BJ. Diet high in fructose promotes liver steatosis and hepatocyte apoptosis in C57BL/6J female mice: role of disturbed lipid homeostasis and increased oxidative stress. *Food Chem Toxicol*. 2017;103:111–21.
25. Priyadarshini E, Anuradha CV. Glucocorticoid antagonism reduces insulin resistance and associated lipid abnormalities in high-fructose-fed mice. *Can J Diabetes*. 2017;41:41–51.
26. Azmi MB, Qureshi SA. *Rauwolfia serpentina* improves altered glucose and lipid homeostasis in fructose-induced type 2 diabetic mice. *Pak J Pharm Sci*. 2016;29:1619–24.
27. Hallfrisch J. Metabolic effects of dietary fructose. *FASEB J*. 1990;4:2652–60.
28. Liu YF, Wei JY, Shi MH, Jiang H, Zhou J. Glucocorticoid induces hepatic steatosis by inhibiting activating transcription factor 3 (ATF3)/S100A9 protein signaling in granulocytic myeloid-derived suppressor cells. *J Biol Chem*. 2016;291:21771–85.
29. Kalfon R, Koren L, Aviram S, Schwartz O, Hai T, Aronheim A. ATF3 expression in cardiomyocytes preserves homeostasis in the heart and controls peripheral glucose tolerance. *Cardiovasc Res*. 2017;113:134–46.
30. Rynes J, Donohoe CD, Frommolt P, Brodesser S, Jindra M, Uhlirova M. Activating transcription factor 3 regulates immune and metabolic homeostasis. *Mol Cell Biol*. 2012;32:3949–62.